1998

Vibration Suppression: Reduced-Order Model/Residual Mode Filter Control Using Smart Structures

Gleave, J.

Vibration Suppression: Reduced-Order Model/Residual Mode Filter Control Using Smart Structures

Janet Gleave Stuart and Brij N. Agrawal
Department of Aeronautics and Astronautics
U.S. Naval Postgraduate School
Monterey, CA 93943-5106
jgstuart@aa.nps.navy.mil agrawal@aa.nps.navy.mil
408-656-2936 408-656-3338

Abstract— For spacecraft with large flexible antennas, and/or flexible support structures, suppressing vibrations caused by on-orbit operational disturbances (e.g., antenna slew maneuvers and thruster firings) is a challenging problem. In the past several years, advances in smart structure technologies have made their use in real-time dynamic control of a structure possible. This paper discusses analytical investigations that are focused on the development of improved vibration suppression techniques for flexible spacecraft structures using smart structure actuators and sensors.

In general, active control of large flexible structures can be used to improve performance, e.g., shape fidelity, line-of-sight pointing accuracy, and vibration and disturbance suppression. Large-scale models of such structures (e.g., finite element models) are appropriate for dynamic simulation but cannot be used as a basis for control algorithms, which must be implemented via computer in real-time. Therefore, control algorithms are often based on *Reduced-Order Models* (ROM) of the structure dynamics. Whenever such a controller operates in closed-loop with the actual structure, unwanted *Controller-Structure Interaction* (CSI) occurs due to un-modeled dynamics. CSI can cause performance degradation and even instability. These instabilities can easily be relieved by the use of low-order *Residual Mode Filters* (RMF). These filters can be added on after the original ROM controller has been designed, and they produce very little degradation of designed performance while yielding an acceptable stability margin for closed-loop operation.

The research presented in this paper integrates smart structure control technologies with the ROM-RMF control technique for active vibration control of a flexible spacecraft structure. This smart structure control technique is applied to a model of the U.S. Naval Postgraduate School's Flexible Spacecraft Simulator (FSS). The FSS simulates motion about the pitch axis of a spacecraft, and is comprised of a rigid central body and a reflector supported by a two-link flexible antenna support structure. The flexible arm representing the antenna support structure has two sets of piezoceramic sensors and actuators, which are used for active vibration control. The ROM-RMF control technique, used in conjunction with optimal control laws, is developed for use with these smart sensors and actuators. The performance of this controller is then compared with the performance of other smart structure controllers previously developed for FSS control.

TABLE OF CONTENTS

1. INTRODUCTION

A current trend in spacecraft design is a movement toward larger, more complex designs, while concurrently reducing the spacecraft's mass to reduce launch costs. The resulting large, lightweight spacecraft are extremely flexible, having low-frequency fundamental vibration modes. These modes are often excited during normal on-orbit operations such as slewing, pointing maneuvers and thruster firings. Effective suppression of this induced vibration is a new and challenging task for spacecraft designers. One promising solution to this design problem is the use of smart structure technologies, including embedded sensors and actuators, and innovative control laws.

In general, smart structures are the system elements that sense the dynamic state and change the system's structural properties (e.g., natural frequencies and damping) to meet given performance objectives. There are several types of embedded sensors and actuators that can be used for vibration suppression and structural control. Embedded sensor candidates are piezoelectric deformation sensors, strain gages, and fiber optic sensors. Embedded actuator candidates are piezoceramic wafers, electrostrictive ceramic wafers, piezoceramic polymer film and shape memory metal wires. This paper focuses on the use of embedded piezoceramic materials for both sensing and actuation in vibration suppression.

Briefly, piezoelectricity is a phenomenon that describes certain materials that generate electricity when a mechanical stress is applied. This is known as the direct piezoelectric

effect. Conversely, when an electric field is applied to these materials a mechanical stress is generated. In this paper, lead zirconate titanate (PZT) piezoceramics are used for both sensing, via the direct effect, and actuation (converse effect) in an experiment to demonstrate their effectiveness in flexible spacecraft vibration suppression.

With respect to the control of smart structures, conventional control methods have worked well in the past. However, new design methods are required to obtain improved performance and robustness characteristics from the structural control system in order to satisfy future design specifications. Positive position feedback (PPF) [1, 2, 3] and velocity feedback are two proven methods of structural control that work well with piezoceramic actuators and sensors. PPF offers quick damping for a particular mode, provided that the modal characteristics are well known, and is also easy to implement. Strain Rate Feedback (SRF) control has also been used for active damping of a flexible space structure [4]. SRF has a wider active damping region and can stabilize more than one mode given a sufficient bandwidth.

The above methods are primarily devised for single-mode vibration suppression, and have limited effectiveness for multi-mode vibration suppression. With a multiple-input-multiple-output (MIMO) control system, linear quadratic control methods are the preferred choice and can be used effectively for multi-mode vibration suppression. Linear Quadratic Gaussian (LQG) design has been applied in smart structure control applications [5, 6, 7]. The control input of LQG is designed to optimize the weighted sum of the quadratic indices of energy (control input) and performance. By adjusting the weights, LQG design can meet a specific requirement, for example, to minimize deflection of a flexible structure. The LQG control approach is well suited for the requirements of damping out the effect of disturbances as quickly as possible and maintaining stability robustness. For this reason, LQG control is utilized in the development of a ROM-RMF smart structure controller in this paper.

Active control of large flexible structures requires the use of reduced-order control algorithms. Inherent in the application of ROM control schemes is the problem of controller-structure interaction (CSI). The issue of CSI is addressed through residual mode filter compensation, which is added onto the ROM controller. The design of the ROM-based control law considers only system performance, while the RMF design insures closed-loop stability.

This paper presents the application of LQG control and ROM-RMF control techniques to vibration suppression of a flexible structure through the use of embedded piezoceramic sensors and actuators. The flexible structure to be controlled is a two-link flexible appendage on the Flexible Space Simulator (FSS) at the U.S. Naval Postgraduate School. With a control objective of minimizing displacement, ROM-RMF control was implemented on the flexible appendage in a cantilevered configuration utilizing piezoelectric sensor output representing structural displacement. Induced vibrations were subsequently controlled through the application of control signals to the embedded piezoelectric actuators. This paper presents the modeling and simulation results for this ROM-RMF control investigation.

2. EXPERIMENTAL SETUP

The Flexible Spacecraft Simulator (FSS), shown in Figure 2.1, simulates motion about the pitch axis of a spacecraft. It is comprised of a single degree-of-freedom rigid central body, representing the spacecraft central body, and a multiple degree-of-freedom, two-link flexible appendage, representing an antenna reflector with a flexible support structure. The flexible appendage is composed of a base beam cantilevered to the main body and a tip beam connected to the base beam at a right angle with a rigid elbow joint. In this experiment, the main body is fixed relative to the granite table and the flexible appendage is floated/supported by one air pad each, at the elbow and tip, and allowed to vibrate freely.

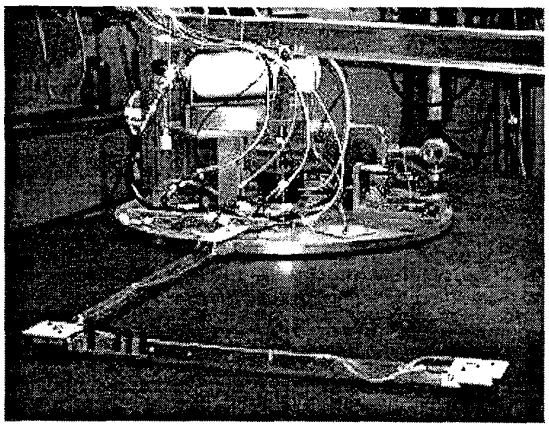

Figure 2.1 Flexible Spacecraft Simulator (FSS)

Piezoceramic sensors and actuators are used to provide active damping to the flexible support structure. The flexible appendage has two stacked piezoceramic pairs as sensor/actuators. The first pair is located at the base of the arm assembly as shown in Figure 2.2. The second pair is located at the base of the forearm near the structure's elbow joint as shown in Figure 2.3.

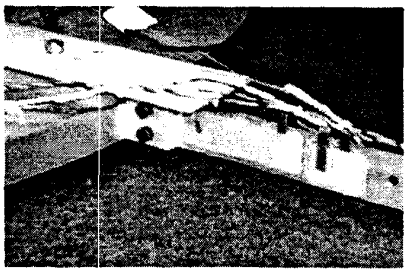

Figure 2.2 Base Piezoceramic Actuator/Sensor Pair

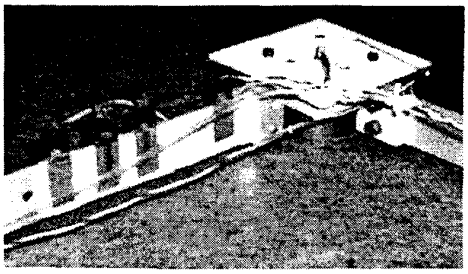

Figure 2.3 Elbow Piezoceramic Actuator/Sensor Pair

3. SYSTEM MODELING

The flexible appendage is modeled [7, 8] using the finite element method. For the analysis, 6 elements were used to characterize the structure. Figure 3.1 shows the element configuration and measurements. Elements 1 and 4 are piezoceramic actuator elements, elements 2 and 5 are piezoceramic sensor elements, and elements 3 and 6 are simple aluminum beam elements. Point masses were added to the elbow joint and tip to represent the connection brackets and air pads. The basic elements were formulated using the direct method of derivation, but were subsequently augmented with the mass and stiffness properties of the piezoelectric patches. Table 3.1 gives the material properties used in modeling the appendage and Table 3.2 gives piezoceramic properties.

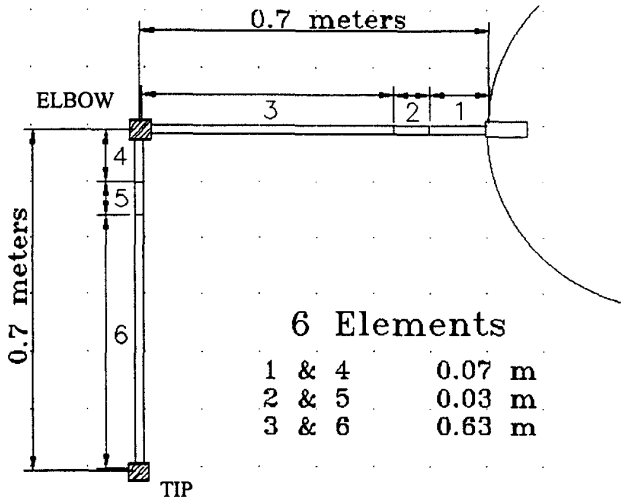

Figure 3.1 FEM Configuration of the Flexible Appendage

Table 3.1 Material Properties of Flexible Appendage

Property	Symbol	Units	Value
Beam thickness	t_b	meters	1.5875×10^{-3}
Beam width	w_b	meters	2.54×10^{-2}
Beam density	ρ_b	kg/m^3	2.800×10^3
Young's Modulus	E_b	N/m^2	1.029×10^7

Table 3.2 Material Properties of Piezoceramics

Property	Symbol	Units	Value
Lateral strain coefficient	d_{31}	*m/V* or *Coul/N*	1.8×10^{-10}
Young's Modulus	E_p	N/m^2	6.3×10^{10}
Poisson's ratio	ν	N/A	0.35
Absolute permittivity	D	*Farad/m* or N/V^2	1.5×10^{-8}

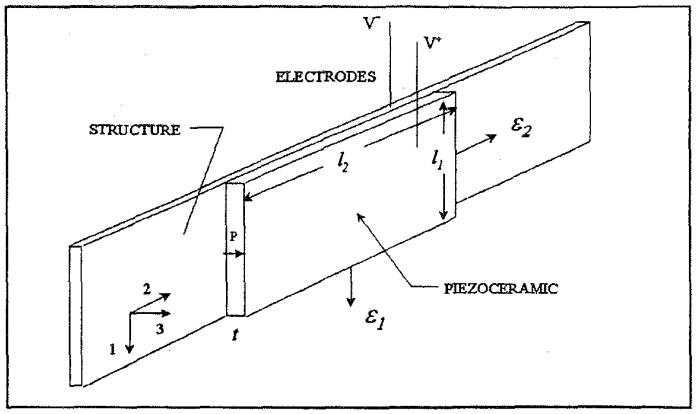

Figure 3.2 Poled Piezoceramic Mounted on FSS Beam

The piezoceramic wafers are bonded to the surface of the flexible arm as shown previously in Figures 2.2 and 2.3. Figure 3.2 illustrates the orientation of a piezoceramic wafer on an arm and the alignment of its poling axis, both of which influence the electro-mechanical relationships. In this smart structure, the voltage developed from the piezoceramic sensors is fed to the piezoceramic actuators by way of the designed control system.

In a sensory mode, the piezoceramic wafers produce a charge, Q, between their electrodes that is directly proportional to the lateral strains and is given by

$$Q = AEd_{31}(\varepsilon_1 + \varepsilon_2) \tag{3.1}$$

where A is the lateral area of the piezoceramic wafer, E is Young's modulus of the wafer, d_{31} is the lateral charge coefficient, and ε_1 and ε_2 are the strain values in the lateral directions. The capacitance, C, for a piezoceramic wafer is given by

$$C = \frac{DA}{t} \tag{3.2}$$

where D is the dielectric constant of the piezoceramic and t is the thickness of the wafer. The voltage V produced by a sensor under strain is given by

$$V = \frac{Q}{C} = \frac{Ed_{31}}{D} t(\varepsilon_1 + \varepsilon_2) \tag{3.3}$$

When using piezoceramic wafers as actuators, the attachment geometry is similar to the sensor geometry shown in Figure 3.2. The control voltage e is applied to the wafers and the lateral strain that is developed can act to control the bending of the beam. The electric field Φ that is developed by the wafer is given by

$$\Phi = \frac{VC}{t} \tag{3.4}$$

The equations of motion for the flexible arm with piezoceramic sensors and actuators are obtained using the finite element method and are in the form

$$[M]\ddot{q} + [K]q = -Be_a \tag{3.5}$$

Where

M = Mass matrix of the beam (including piezoceramics)
K = Stiffness matrix of the beam (including piezoceramics)
q = Generalized coordinate vector (representing translational & rotational motion at nodes)
B = Actuator influence vector (representing locations of actuators)
e_a = Applied actuator voltage vector (representing actuator inputs)

For the piezoceramic sensor, the equation is

$$e_s = \frac{1}{\gamma} B^T q \tag{3.6}$$

Where

e_s = Output sensor voltage vector
B^T = Sensor influence vector (representing locations of sensors)
γ = Coefficient representing piezoceramic parameters

The next step is the development of a ROM-RMF control law that determines the voltage applied to the actuators as a function of sensor output and the measured and estimated states of the structure.

4. ROM-RMF CONTROL

In designing a controller for flexible structures, certain system modes are extremely important in the overall performance of the structure. A *reduced-order model* (ROM) based control focuses on these modes, providing a viable active control algorithm for large systems. Unfortunately, un-modeled structural dynamics can interact with the ROM controller, through *controller-structure-interaction* (CSI) and cause crippling deterioration of system performance, possibly to the point that system stability is lost. A *residual mode filter* (RMF) eliminates one channel of CSI, while adding only a simple, second-order filter to the control loop. Thus, the ROM controller can be designed separately, based strictly on performance criteria. Residual mode filters can then be selected to compensate for CSI as needed.

A fundamental advantage of ROM-RMF design is its straightforward methodology [9, 10, 11]. The design advances from one stage to the next without iteration, and the controller is constructed incrementally. To begin, a reduced-order model is assembled. A variety of techniques may be used to generate a suitable ROM, but in this paper a modal reduction scheme is used. Given a modal representation of the system, the modes important for performance are selected. These modes make up the ROM, while all others are defined as residual modes. The only constraint on the ROM is that it contains all rigid body modes of the plant.

The controller is designed to tailor the output of the ROM modes to meet performance specifications. However, communication between the plant and the controller occurs through actuators and sensors, and is therefore non-modal. As shown in Figure 4.1, actuators pump energy into all modes and sensors cannot distinguish modal data. Since the control model includes no information about residual modes, the ROM controller may be unstable in closed-loop with the plant. Even if controller-structure interaction is not severe enough to destabilize the feedback system, it will reduce system performance, possibly below acceptable limits.

In the next stage of design, the closed-loop system is analyzed for stability. Assume here that CSI degrades the system's response inadmissibly, since if this were not the case, controller design would be finished. From the analysis, one can distinguish the residual modes that interact most acutely with the ROM-based controller; call these modes Q-modes. The residual mode filter is designed to reproduce modal data using knowledge of the Q-modes, and the measured output of the system. Exploiting this information, the input to the ROM control is screened via a RMF added around the controller, as shown in Figure 4.2. The RMF design proceeds independently from the design for performance, and thus requires no redesign of the ROM controller.

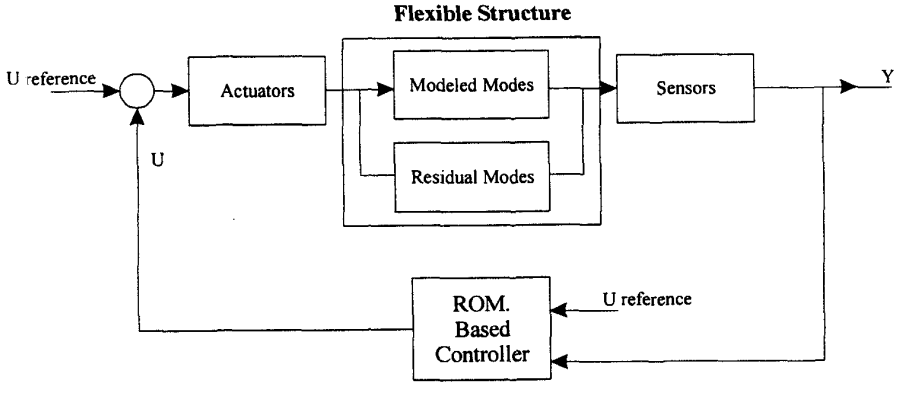

Figure 4.1 ROM-Based Control of Flexible Structures

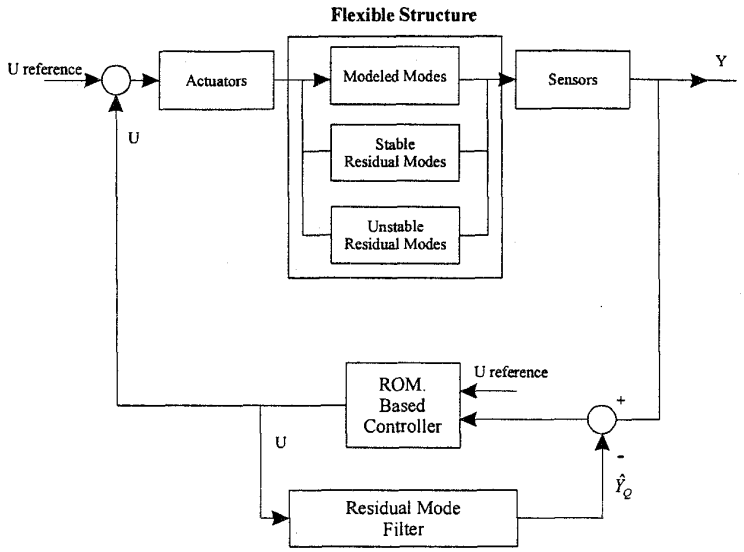

Figure 4.2 ROM-RMF Control of Flexible Structures

Though designed after the ROM controller to stabilize the closed-loop system, the RMF is not a "patch." Rather, analysis shows the RMF to be a simple extension of the state observer [12]. RMF compensation makes better use of whatever knowledge there is of the plant through a small addition to the ROM controller. Thus, ROM-RMF design guides the splitting of a single, complicated problem (design for stability and performance) into its component parts, while guaranteeing stable, ROM-based control.

State Space Representation

As discussed in the previous section, a modal description of the system is required for the implementation of ROM control. In this case, modes are determined via finite element analysis of the FSS. Solution of the eigenvalue problem using the finite element model discussed in Section 3 yielded 12 modes and mode shapes. Table 4.1 lists the first 6 frequencies of oscillation and Figure 4.3 shows the first 2 mode shapes. These two modes are the primary carriers of energy for the structure, and will be included in the ROM and actively controlled.

Table 4.1 Natural Frequencies of Flexible Arm Model

Mode	Frequency (Hz)
1	0.29583
2	0.87067
3	11.108
4	28.496
5	45.144
6	102.78

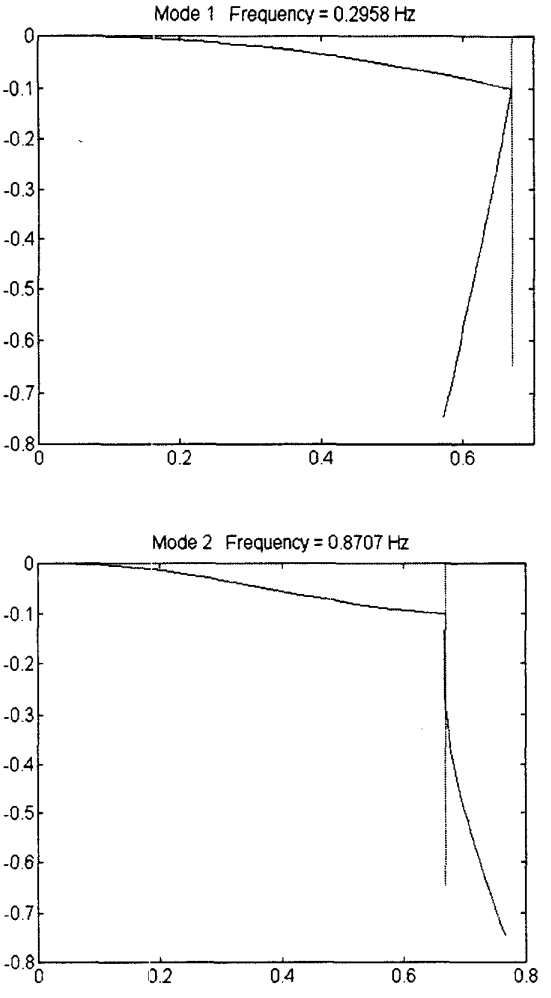

Figure 4.3 The First Two Mode Shapes for the Flexible Appendage

In the absence of the external input, the system dynamics are governed by

$$[M]\ddot{q} + [K]q = 0$$

The desired equations of motion are of the form

$$[M]\ddot{q} + [C]\dot{q} + [K]q = 0 \tag{4.1}$$

where $[C]$ is the damping matrix for the system in physical coordinates. Utilizing the linear similarity transformation

$$q = S\Psi, \quad T = S^{-1}, \quad S = Tq \tag{4.2}$$

where S is chosen so that

$$S^T[M]S = I$$

$$S^T[C]S = \text{diag}(\cdots, \quad 2\varsigma\omega_i, \quad \cdots) = [\Omega]$$

$$S^T[K]S = \text{diag}(\cdots, \quad \omega_i^2, \quad \cdots) = [\Lambda]$$

Eqn. (4.1) can be transformed into a diagonal form in terms of the modal coordinate vector, Ψ

$$\ddot{\Psi} + [\Omega]\dot{\Psi} + [\Lambda]\Psi = 0 \tag{4.3}$$

which can be rewritten in state space form

$$\begin{Bmatrix} \dot{\Psi} \\ \ddot{\Psi} \end{Bmatrix} = A_m \begin{Bmatrix} \Psi \\ \dot{\Psi} \end{Bmatrix} \tag{4.4}$$

where

$$A_m = \begin{bmatrix} 0 & I \\ -[\Lambda] & -[\Omega] \end{bmatrix}$$

The system (4.4) can be transformed back to the physical coordinates by utilizing $S = Tq$,

$$\begin{Bmatrix} \dot{q} \\ \ddot{q} \end{Bmatrix} = A \begin{Bmatrix} q \\ \dot{q} \end{Bmatrix} \tag{4.5}$$

where

$$A = \begin{bmatrix} T & 0 \\ 0 & T \end{bmatrix}^{-1} A_m \begin{bmatrix} T & 0 \\ 0 & T \end{bmatrix}$$

Considering the external inputs, and both state noise and sensor noise, Eqn. (4.5) can be rewritten in standard state space form as

$$\dot{x} = Ax + Bu + Fw \tag{4.6a}$$

$$y = Cx + v \tag{4.6b}$$

where $x = \{q^T, \dot{q}^T\}^T \in \Re^{24}$ represents the translational and rotational displacements and velocities

at node points of the finite element model. $u \in \Re^2$ denotes the control voltages of the base and elbow actuators. $y \in \Re^2$ is the sensor output vector, which consists of two piezoceramic sensor output voltages. $B \in \Re^{24\times 2}$ is the input matrix. $C \in \Re^{2\times 24}$ is the output matrix. $v \in \Re^2$ represents the measurement noise. F is the plant uncertainty matrix and w is the state noise vector. The states are estimated using a Kalman filter.

Linear Quadratic Gaussian Control

To minimize displacement of the flexible appendage, the Linear Quadratic Gaussian (LQG) method is used. The control voltages for the actuators are determined by the optimal control solution of the Linear Quadratic Regulator (LQR), which is an effective and widely used linear control technique. Provided the full state vector is observable, this method can be employed to meet specific design and performance criteria. A quadratic cost function is used to minimize the performance index, J. The general form for the LQR is

$$J = \int \left(x^T Q x + u^T R u\right) dt \tag{4.7}$$

where Q is the state weighting matrix, and R is the control weighting matrix. The solution to the LQR problem seeks a compromise between minimum energy (control input) and best performance.

The weighting scheme used was approximately $Q_N = diag[\Lambda_N, I_N]$ so that $E_N = x_N{}^T Q_N x_N$ is the energy in the controlled modes. The weighting values of R are selected such that the control input voltage to the actuators is within their limitations of 150 volts, or $R = 0.1 * I$. The control voltage is obtained according to

$$u = -K_{LQR} x = -R^{-1} B^T G x \tag{4.8}$$

where G is the solution to the Riccati equation

$$-Q - A^T G - GA + GBR^{-1} B^T G = 0$$

The Kalman filter is designed as

$$\dot{\hat{x}} = (A - BK_{LQR} - \hat{L}C)\,\hat{x} + \hat{L} y \tag{4.9}$$

where the optimum observer gain $\hat{L}$ is given by

$$\hat{L} = \hat{P} C' W^{-1} \tag{4.10}$$

with $\hat{P}$ defined as

$$\dot{\hat{P}} = A\hat{P} + \hat{P}C^T - \hat{P}\,C^T W^{-1} C\,\hat{P} + FVF^T$$

where the process noise covariance matrices V and W are given by

$$E\{vv^T\} = V(t)\,\delta(t-\tau)$$
$$E\{vw^T\} = X(t)\,\delta(t-\tau)$$
$$E\{ww^T\} = W(t)\,\delta(t-\tau)$$

and $X(t)$ is the system cross-covariance matrix, which is a function of the correlation of sensor noise to plant noise. (Under most circumstances $X(t)$ is normally zero). $E\{\}$ denotes mathematical expectation.

ROM Controller Design

In the development of a ROM controller, N-modes are selected for inclusion in the ROM and the states of the system, as given in Eqn. 4.6, are partitioned according to

$$x = \begin{Bmatrix} x_N \\ x_R \end{Bmatrix} \tag{4.11}$$

where R denotes the number of residual modes. In this control investigation N=2, corresponding to a ROM based on the first two low-frequency modes of the system. Assuming for the time being that plant uncertainty and state and measurement process noise in Eqn. 4.6 are negligible, the state equations can be written in partitioned form according to

$$\dot{x}_N = A_N x_N + B_N u$$

$$\dot{x}_R = A_R x_R + B_R u \tag{4.12}$$

$$y = y_N + y_R = C_N x_N + C_R x_R$$

Modal information for the N-critical modes can be used to assess the controllability and observability of the ROM (A_N, B_N, C_N). For this particular configuration of the FSS (i.e., fixed central body and given piezoelectric actuator and sensor locations) the system was found to be controllable, but not observable. However, the conditions for a unique positive definite solution to the LQR problem were met (i.e., Q symmetric and positive semi-definite, R symmetric and positive definite and (A_N, B_N) controllable). For the research presented here, a ROM-based state estimator was used in lieu of the Kalman Filter in (4.9) and (4.10). However, since (A_N, C_N) was not observable, there was some difficulty placing the poles of the estimator to the left of the poles of the regulator in the left-half-plane, as is typically desired in control system design.

The ROM-based state estimator is given by

$$u = G_N \hat{x}_N \tag{4.13}$$

$$\dot{\hat{x}}_N = A_N \hat{x}_N B_N u + K_N (y - \hat{y}_N)$$

$$\hat{y}_N = C_N \hat{x}_N$$

where $G_N = -K_{LQR}$ in (4.8) and the estimator error, $e_N \equiv \hat{x}_N - x_N$, satisfies

$$\dot{e}_N = (A_N - K_N C_N) e_N + K_N C_R x_R \tag{4.14}$$

Defining $w = \begin{bmatrix} x_N \\ e_N \\ x_R \end{bmatrix}$, the closed-loop system is now

$$\dot{w} = A_C w \tag{4.15}$$

where

$$A_c \equiv \begin{bmatrix} A_N + B_N G_N & B_N G_N & 0 \\ 0 & A_N - K_N C_N & K_N C_R \\ B_R G_N & B_R G_N & A_R \end{bmatrix} \tag{4.16}$$

Uncompensated ROM Controller Performance

There are various techniques, such as perturbation theory, for determining the stability of A_c in the presence of observation spillover ($K_N C_R$) and control spillover ($B_R G_N$). In this case, however, the dimension of A_c is not prohibitively large and the eigenvalues are computed directly using MATLAB. In this case, all eigenvalues are in the left-half-plane and the system is stable, even in the presence of spillover. Simulations for the open-loop ROM and closed-loop ROM systems were conducted. Figures 4.4 and 4.5 show the impulse responses for the open-loop ROM and the closed-loop ROM systems, respectively, and demonstrate the effectiveness of ROM control in this application. Note that the time scales are the same in Figures 4.4 and 4.5, but that the open-loop system took about 120 seconds for the output to damp out and go to zero (not shown). The simulation of the ROM-based controller shows a marked improvement over open-loop performance. As mentioned previously, the uncompensated ROM controller was stable in the presence of observation and control spillover. The impulse response for this uncompensated system is shown in Figure 4.6. The performance of the uncompensated ROM controller is virtually the same as the closed loop ROM controller, and in this instance, the addition of a RMF would only minimally increase controller performance.

A Few Words about Residual Mode Filters

Although the use of a residual mode filter is not warranted here, some of the techniques [13] for identifying troublesome modes, or Q-modes, are relevant. The Q-mode selection process is not an exact science and is based on performance measures and rules of thumb. One useful indicator is the relative magnitudes of ($K_N C_R$), or the observation spillover, for the residual modes. For the 2-mode ROM presented here, this indicator identified the second residual mode (mode 4 from Table 4.1) as a possible troublesome mode since it was the only residual mode with non-zero elements in ($K_N C_R$). This particular residual mode also had relatively high values of control spillover in ($B_R G_N$). The spillover effects for this residual mode, as well as the others, did not *significantly* degrade performance and a RMF is not required. However, if the ROM controller is subsequently redesigned to increase performance, this modal information will be useful in designing and implementing a RMF if required. And finally, the residual mode information from this investigation has led to subsequent research featuring a 1-mode ROM controller.

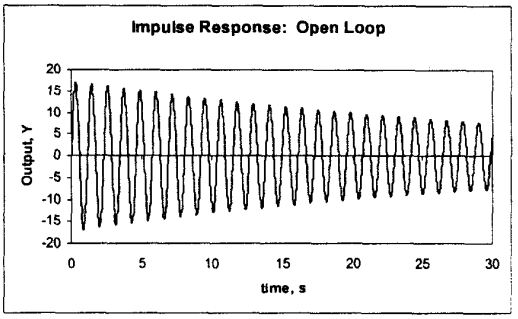

Figure 4.4 Impulse Response: Open-Loop ROM

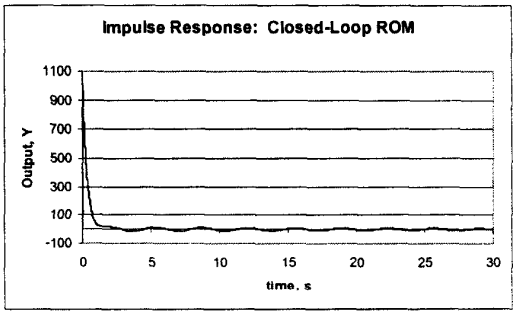

Figure 4.5 Impulse Response: Closed-Loop ROM

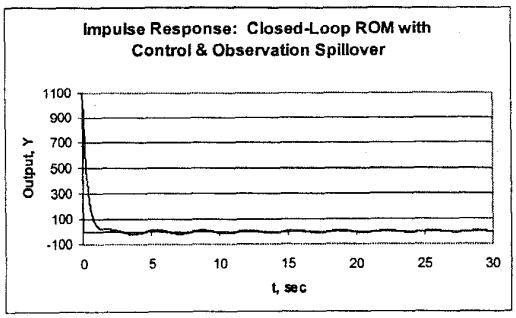

Figure 4.6 Impulse Response: Closed-Loop ROM with Observation and Control Spillover

5. CONCLUSIONS

This paper presented an analytical investigation that focused on the development of improved vibration suppression techniques for flexible spacecraft structures using smart structure actuators and sensors. The effectiveness of *reduced-order model* (ROM) control in multi-mode vibration suppression of the Naval Postgraduate School's Flexible Spacecraft Simulator (FSS) was demonstrated. A finite element model of the FSS was presented and subsequently used to develop a 2-mode ROM of the FSS using the first two low-frequency modes of the system. LQG techniques were used for ROM controller gain selection. Simulations of the resulting ROM-control system showed marked improvement over the performance of the open-loop system, and stable closed-loop performance in the presence of observation and control spillover. This spillover is a result of interaction of the un-modeled dynamics of the flexible structure with the controller, but was not significant enough to necessitate the use of a *residual mode filter* (RMF) in this control investigation. The performance of the ROM controller, although preliminary, compares favorably with other smart structure control techniques and will be implemented in a subsequent experimental control investigation using the FSS in the near future.

ACKNOWLEDGEMENTS

This paper is based on research performed in the Spacecraft Attitude Dynamics and Control Laboratory (www.aa.nps.navy.mil/~spacelab/) at the Naval Postgraduate School under a National Research Council grant. The authors would like to sincerely acknowledge the significant contributions of previous FSS researchers, especially LtCDR W.B. Harrington and Dr. G. Song.

REFERENCES

[1] C.J. Goh and T.K. Caughey, "On the Stability Problem Caused by Finite Actuator Dynamics in the Collocated Control of Large Space Structure," Int. J. Control, Vol. 41, No. 3, 1985, pp.787-802.

[2] J.L. Fanson and T.K. Caughey, "Positive Position Feedback Control for Large Space Structure," AIAA Journal, Vol. 28, No. 4, April, 1990, pp.717-724.

[3] B.N. Agrawal and H. Bang, "Adaptive Structure for Large Precision Antennas," 45th Congress of the International Astronautical Federation (Jerusalem, Israel), October, 1994.

[4] S.M. Newman, "Active Damping Control of a Flexible Space Structure Using Piezoelectric Sensors and Actuators," Master Thesis, U.S. Naval Postgraduate School, December, 1992.

[5] C.C. Won, J.L. Sulla, D.W. Sparks Jr. and W.K. Belvin, "Application of Piezoelectric Devices to Vibration Suppression," Journal of Guidance, Control, and Dynamics, Vol. 17, No. 6, November

[6] B.N. Agrawal, "Spacecraft Vibration Suppression Using Smart Structures," Fourth International Congress on Sound and Vibration (St. Petersburg, Russia), June, 1996, pp. 563-570.

[7] W.B. Harrington, Jr., "Optimal Linear Quadratic Gaussian Controller Design for a Flexible Spacecraft Simulator," M.S. Thesis, Naval Postgraduate School, December, 1995.

[8] W.B. Harrington, Jr., "Experimental Verification of an Optimal Linear Controller for a Flexible Structure," Engineer Thesis, Naval Postgraduate School, December, 1995.

[9] M.J. Balas, "Feedback Control of Flexible Structures," IEEE Transactions on Automatic Control, vol. AC-23, no. 4, pp. 673-679, 1978.

[10] M.J. Balas, Mechanics and Control of Large Flexible Structures (Chapter 11), Washington DC, American Institute of Aeronautics and Astronautics, Inc., 1990, pp. 295-313.

[11] B.T. Reisenauer, C.S.I. Compensation for Reduced-Order Model Based Control of a Flexible Robot Manipulator, M.S. Thesis, University of Colorado at Boulder, Department of Aerospace Engineering Sciences, 1990.

[12] M.J. Balas, R. Quan, R. Davideson, B. Das, "Low-Order Control of Large Aerospace Structures Using Residual Mode Filters," Proc. Of ACC, 1988.

[13] J.G. Stuart, Distributed Parameter Control of a Large, Flexible Stiff-Membrane Phased Array Using Thin-Film Piezoelectric Actuator Patches, Ph.D. Thesis, University of Colorado at Boulder, Department of Aerospace Engineering Sciences, 1995.

Janet Gleave Stuart *is currently a National Research Council Fellow at the Naval Postgraduate School in Monterey, CA, where she is conducting research in the area of flexible spacecraft structural control using smart structure technologies. Prior to her appointment at the Naval Postgraduate School, Dr. Stuart performed postdoctoral research in the areas of flexible rotor dynamics and control, and smart-rotor/adaptive-rotor active control systems. This research was sponsored by the U.S. Department of Energy's National Renewable Energy Laboratory/ National Wind Technology Center in Golden, CO. Dr. Stuart previously worked as an engineer at Honeywell Satellite Systems in the area of control moment gyros and reaction wheel systems, and at the Lawrence Livermore National Laboratory, in the area of space-based energy systems. She has also consulted for various satellite telecommunications companies, including Leo One Panamericana, of Mexico City, Mexico, and Teledesic, Corp., of Kirkland, WA, and has over twenty technical publications. She received her B.S. in Mechanical Engineering from Utah State University in 1987, a M.S. in Aerospace Engineering Sciences from the University of Colorado at Boulder in 1990, and her Ph.D. in Aerospace Engineering Sciences, also from the University of Colorado at Boulder, in 1995. She also attended the International Space University in Kitakyushu, Japan in 1992.*

Dr. Brij N. Agrawal is a Professor in the Department of Aeronautics and Astronautics and Director of the Spacecraft Research and Design Center. Professor Agrawal came to NPS in 1989 and has since initiated a new M.S. curriculum in Astronautical Engineering in addition to establishing the Spacecraft Research and Design Center. He has also developed research programs in attitude control of flexible spacecraft, "Smart" structures, and space robotics. Prior to NPS he worked for Communications Satellite Corporation (COMSAT) and International Telecommunications Satellite Organization (INTELSAT) where he conducted research in spacecraft attitude dynamics, structural dynamics, and spacecraft testing. He has participated in the development of INTELSAT IV, IV-A, V, VI, and VII, COMSTAR, and MARISAT satellites. Professor Agrawal has written an industry recognized textbook "Design of Geosynchronous Spacecraft", has over 40 technical papers, and has a patent for an attitude pointing error correction system for geosynchronous satellites. Professor Agrawal received his Ph.D. in Mechanical Engineering from Syracuse University in 1970 and his M.S. in Mechanical Engineering from McMaster University in 1968. He has received the NPS Outstanding Teacher Award, an AIAA Space Design Award, and the INTELSAT Award for Inventiveness and Technological Contribution. Professor Agrawal is an Associate Fellow of the American Institute of Aeronautics and Astronautics and a registered P.E. in the state of Maryland.